ELSEVIER

Journal of Organometallic Chemistry 530 (1997) 27–38

Journal of Organometallic Chemistry

New organogold(I) complexes: synthesis, structure, and dynamic behavior of the polynuclear organogold diphenylmethane and diphenylethane derivatives

Tat'yana V. Baukova [a,*], Lyudmila G. Kuz'mina [b], Natal'ya A. Oleinikova [a], Dmitrii A. Lemenovskii [c], Aleksander L. Blumenfel'd [a]

[a] Nesmeyanov Institute of Organoelement Compounds, Russian Academy of Science, Vavilov St. 28, Moscow 117813, Russia
[b] Kurnakov Institute of General and Inorganic Chemistry, Russian Academy of Science, Leninskii pr. 31, Moscow 117907, Russia
[c] Chemistry Department, Moscow State University, Leninskie Gory, Moscow 117234, Russia

Received 9 March 1996; revised 24 May 1996

Abstract

Two organogold derivatives of diphenylmethane and diphenylethane, $Ph_3PAu(o\text{-}C_6H_4)CH_2(C_6H_4\text{-}o)AuPPh_3$ (**1**) and $Ph_3PAu(o\text{-}C_6H_4)(CH_2)_2(C_6H_4\text{-}o)AuPPh_3$ (**2**), have been synthesized by the reaction of $ClAuPPh_3$ with $Li(o\text{-}C_6H_4)CH_2(C_6H_4\text{-}o)Li$ and $Li(o\text{-}C_6H_4)(CH_2)_2(C_6H_4\text{-}o)Li$ respectively. The interaction of **1** with dppe results in the replacement of the two PPh_3 groups to give a macrocyclic compound $Au(o\text{-}C_6H_4)CH_2(C_6H_4\text{-}o)Au(\mu\text{-}PPh_2CH_2CH_2PPh_2)$ (**3**) that includes an Au ··· Au bond. Compounds **1** and **2** react with one or two equivalents of $[Ph_3PAu]BF_4$ to form new types of cationic complex $[CH_2(C_6H_4\text{-}o)_2(AuPPh_3)_3]BF_4$ (**4**), $[CH_2(C_6H_4\text{-}o)_2(AuPPh_3)_4](BF_4)_2$ (**5**), and $[(CH_2)_2(C_6H_4\text{-}o)_2(AuPPh_3)_4](BF_4)_2$ (**6**). Complexes **1–6** have been characterized by X-ray diffraction studies, FAB MS, and IR as well as by ^1H and ^{31}P NMR spectroscopy. A complicated system of Au ··· H–C agostic interactions, involving the bridging alkyl groups ($-CH_2-$ and $-CH_2-CH_2-$) of diphenylmethane and diphenylethane ligands, has been found to occur in complexes **1–3** and **6**.

Keywords: Agostic; Fluxionality; Crystal structure; Phenyl; Gold; Phosphine

1. Introduction

In the last ten years, a large number of secondary bonding interactions has been discovered for gold(I) compounds of general type R–Au–L where R is an organic radical and L a phosphine ligand. The following types of secondary bond are most abundant: Au ··· X (where X is a heteroatom) [1–3], Au ··· H–C (the agostic bond) [4,5], Au ··· π-system [6–8], and Au ··· Au [9–14]. Of these, the Au ··· X bonds are the most investigated [1–3]. The nature of the Au ··· Au bond remains a fascinating problem [15–17].

Different secondary bonds observed in gold(I) compounds are responsible for their uncommon structures and reactivities. It is of interest that some of these structures resemble those previously postulated as unstable intermediates or transition states in reactions of complexes of other metals. Therefore, an investigation of different kinds of secondary bond is very important not only for the development of gold chemistry but also for organometallic and cluster chemistry as a whole.

A new way of investigating secondary bonds that we have developed is the use of specially designed molecules where competition for various secondary bonds within a molecule can occur due to their conformational flexibility. This method offers possibilities of controlling structures and reactivities of the compounds through the variation of different structural fragments in the framework of the model molecule.

Our recent investigations have shown that quite different coordination modes of the organic ligand can occur in two rather closely related 2,2′-diaurated derivatives of the diaryl series: the diphenyl complex $Ph_3PAu(o\text{-}C_6H_4)(C_6H_4\text{-}o)AuPPh_3$ (**7**) and the diphenyloxide complex $Ph_3PAu(o\text{-}C_6H_4)O(C_6H_4\text{-}o)AuPPh_3$ (**8**). According to an X-ray diffraction study,

* Corresponding author.

PII S0022-328X(96)06539-4

a structure with an Au ··· Au bond (3.02 Å) occurs in **7** [18]. The introduction of the oxygen atom between the two aurated phenyl rings in molecule **7** results in a structure for **8** with the gold atoms spaced further from one another. The interaction of both gold atoms with two lone electron pairs of the oxygen atoms rather than with one another causes an additional stabilization of complex **8** [19].

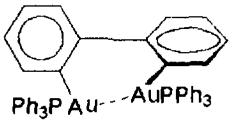

(7)

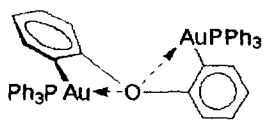

(8)

In this paper, we report the synthesis and structural characterization of new polynuclear organogold derivatives of diphenylmethane and diphenylethane.

2. Results and discussion

2.1. Synthesis and structure of the $Ph_3PAu(o\text{-}C_6H_4)CH_2(C_6H_4\text{-}o)AuPPh_3$ (1) and $Ph_3PAu(o\text{-}C_6H_4)(CH_2)_2(C_6H_4\text{-}o)AuPPh_3$ (2) complexes

Binuclear organogold(I) 2,2′-derivatives of diphenylmethane **1** and diphenylethane **2** were obtained by interaction of $ClAuPPh_3$ with $Li(o\text{-}C_6H_4)CH_2(C_6H_4\text{-}o)Li$ or $Li(o\text{-}C_6H_4)CH_2CH_2(C_6H_4\text{-}o)Li$ in ether–THF medium (Eqs. (1) and (2)).

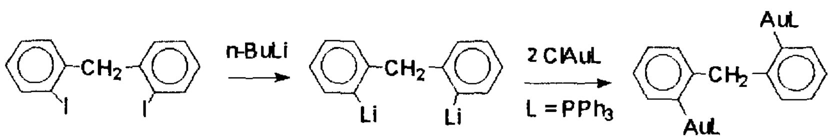

1 (64%)

(1)

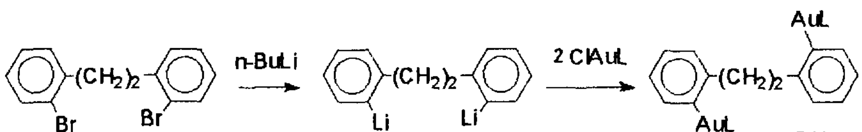

2 (51%)

(2)

In both cases, the dilithium derivatives of diphenylmethane and diphenylethane were synthesized from the corresponding 2,2′-dihalogenated hydrocarbons. These Li_2-derivatives were added to $ClAuPPh_3$ without any special purification. It was found that some excess of the dilithium reagent was required in the syntheses of **1** and **2**.

Compounds **1** and **2** are colorless crystalline substances, soluble in benzene, THF, and chloroform. The structures **1** and **2** were determined by X-ray diffraction studies. Some further details of chemical and structural characterizations of **1** and **2** in the gaseous state or in solution were established by FAB MS, as well as by ^1H and ^{31}P NMR spectroscopy.

2.2. Comparative X-ray structures of complexes 1 and 2

The main data for the crystal structure of **1** were published earlier [20]. The molecular structure of **1**, $Ph_3PAu(o\text{-}C_6H_4)CH_2(C_6H_4\text{-}o)AuPPh_3$, is shown in Fig. 1.

In the solid state complex **1** has a *trans*-type conformation of 2,2′-diaurated phenyl fragments, whereby the gold atoms are separated from one another by 5.631 Å. Such a conformation prevents a direct interaction between the gold atoms.

The actual conformation of molecule **1** (the C(8) ··· C(13) ring is near coplanar to the central C(8)C(7)C(6) plane, whereas another ring, C(1) ··· C(6), is rotated from this plane by 108.5°) is such that both gold atoms approach the hydrogen atoms at the methylene bridge. There are three short distances: Au(1) ··· H(7B) 3.01, Au(2) ··· H(7A) 2.92, and Au(2) ··· H(7B) 3.06 Å. All of these distances can be considered as weak agostic interactions. The formation of an agostic bonding to Pd(II) and Pt(II) with two or three methane hydrogen atoms has been suggested by quantum-chemical calculations [21].

Fig. 2 illustrates the molecular structure of $Ph_3PAu(o\text{-}C_6H_4)(CH_2)_2(C_6H_4\text{-}o)AuPPh_3$ (**2**). The molecule lies on a center of symmetry. Selected bond lengths and bond angles are given in Table 1.

In the crystal, molecule **2** adopts an *anti* conformation with respect to the central ethylene group, a conformation where the gold atoms are well separated.

The planes of benzene rings are rotated around the $C(H_2)$–C(Ph) bonds with respect to the central CCCC plane that includes the phenyl C(*ipso*) atoms and the C

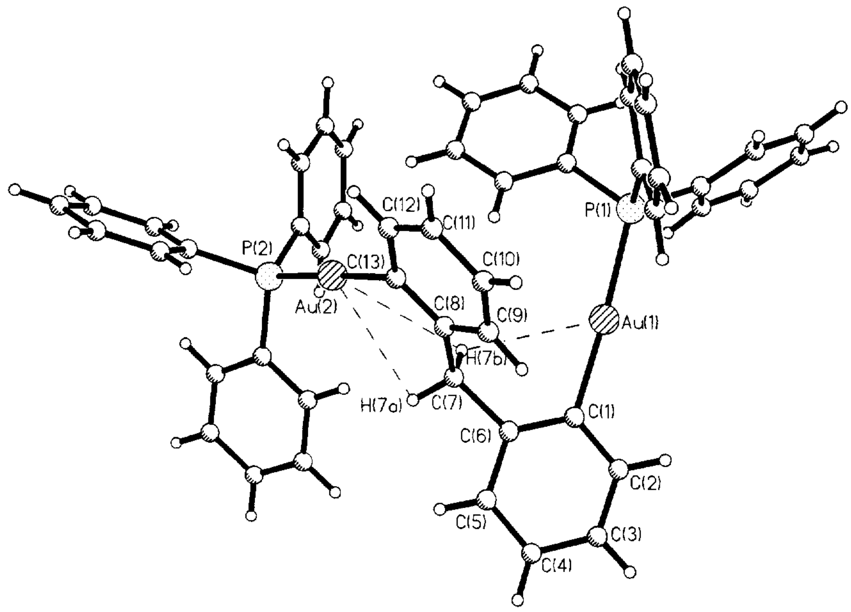

Fig. 1. The molecular structure of $Ph_3PAu(o\text{-}C_6H_4)CH_2(C_6H_4\text{-}o)AuPPh_3$ (**1**).

atoms of the CH_2 groups; the dihedral angle is 78.4°. In the ligand, such an orientation of the benzene rings corresponds to minimum steric interactions between the ethylene and phenyl fragments. In contrast, in this conformation each gold atom approaches the hydrogen atoms of the ethylene bridge. One Au · · · H contact with the hydrogen atom nearest to a particular gold atom (2.75 Å) and another one with more distant ethylene hydrogen (3.00 Å) can correspond to the weak agostic bonds.

It was of interest to establish whether complexes **1** and **2** can adopt another conformation with the direct Au · · · Au intramolecular secondary bond. Our molecular mechanic calculations [20] performed for **1** and **2** skeletons showed that, in both complexes, no steric restrictions for such a conformation exist. The actual conformations of the organic ligands, along with those allowing for the direct Au · · · Au bond in these molecules, are among the most sterically favorable ones. Therefore, complexes **1** and **2** are interesting new models for the comparative investigation of the different types of secondary bond.

Thus, the conformations favorable for weak agostic interactions rather than that with an Au · · · Au bond were found for molecules **1** and **2** in the crystal state.

2.3. Spectral parameters of complexes 1 and 2

The IR spectra of **1** and **2** (in the solid state) exhibit noticeable shifts (by approximately 100 cm^{-1}) of the stretching vibration bands of the CH bonds to low frequency (2870 and 2700 cm^{-1}) compared with those in diphenylmethane (or 2,2′-diiododiphenylmethane) and diphenylethane, an observation which is characteristic of an M · · · H–C agostic bond [22].

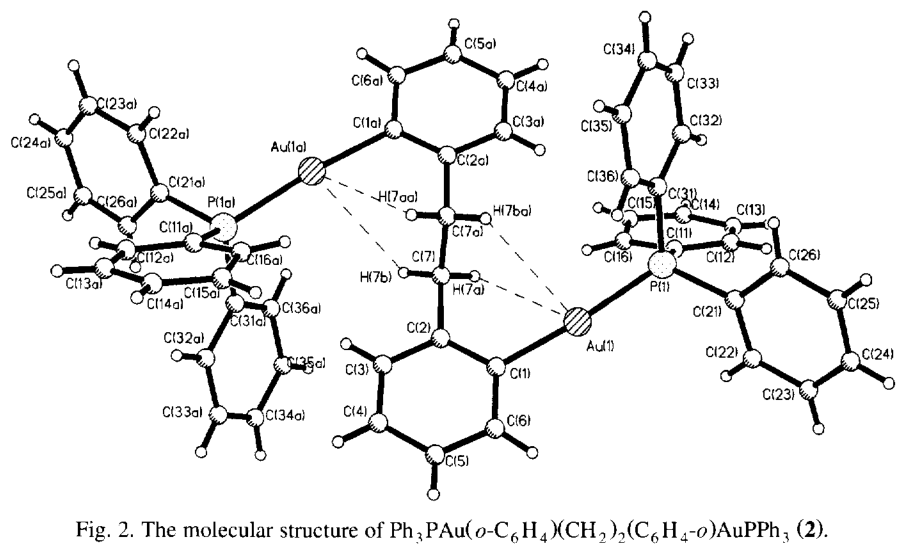

Fig. 2. The molecular structure of $Ph_3PAu(o\text{-}C_6H_4)(CH_2)_2(C_6H_4\text{-}o)AuPPh_3$ (**2**).

Table 1
Selected bond lengths (*d*, Å) and angles (*ω*, deg) for **2**

Bond	*d*
Au(1)–C(1)	2.05(2)
Au(1)–P(1)	2.279(8)
Au(1)···H(7a)	2.75
Au(1)···H(7ba)	3.00
C(1)–C(6)	1.39(2)
C(1)–C(2)	1.39(2)
C(2)–C(3)	1.39(3)
C(2)–C(7)	1.52(3)
C(3)–C(4)	1.39(2)
C(4)–C(5)	1.40(3)
C(5)–C(6)	1.41(3)
C(7)–C(7A)	1.51.(6)
Angle	***ω***
C(1)–Au(1)–P(1)	174.5(5)
C(6)–C(1)–C(2)	120(1)
C(6)–C(1)–Au(1)	123(1)
C(2)–C(1)–Au(1)	117(1)
C(3)–C(2)–C(1)	120(2)
C(3)–C(2)–C(7)	118(2)
C(1)–C(2)–C(7)	122(2)
C(4)–C(3)–C(2)	121(1)
C(3)–C(4)–C(5)	119(2)
C(4)–C(5)–C(6)	120(2)
C(1)–C(6)–C(5)	120(2)
C(7A)–C(7)–C(2)	116(3)

In the temperature range +25 to −95 °C, the ^{31}P NMR spectrum of **1** contains a sharp signal from the two equivalent phosphorus nuclei at $\delta = 43.68$ ppm. The spectrum of complex **2** contains a signal at 44.18 ppm.

The ^{1}H NMR spectra of **1** and **2** in CD_2Cl_2 at room temperature exhibit a sharp singlet assigned to methylene (for **1**) or ethylene (for **2**) protons (4.68 ppm or 3.35 ppm respectively), significantly shifted to low field compared with that of free diphenylmethane (4.00 ppm) or diphenylethane (2.87 ppm); complex multiplets of phenyl protons of **1** and **2** also occur in the aromatic regions.

Temperature dependence of the ^{1}H NMR spectra of **1** and **2** is observed in the range +25 to −90 °C. In the temperature range +25 to −5 °C the ^{1}H NMR spectra indicate a stereochemical non-rigidity of molecules **1** and **2**, caused by rotation of the gold-containing phenyl fragments around the C–C exocyclic bonds of $Ph_3PAuC_6H_4–CH_2–C_6H_4AuPPh_3$ (**1**) and $Ph_3PAuC_6H_4–CH_2–CH_2–C_6H_4AuPPh_3$ (**2**) or by intramolecular vibrations resulting in the effective averaging of their positions against the gold atom. In the range +25 to −4 °C the protons of the CH_2 groups give a sharp singlet. Lowering the temperature to −90 °C (further cooling of the sample under investigation in CD_2Cl_2 is impossible) slows down the dynamic processes and results in some magnetic non-equivalence of the protons. These processes are accompanied by a significant broadening of the signals of the CH_2 or $(CH_2)_2$ group (in **1** or **2** respectively) and their noticeable high field shifts to 4.55 and 3.08 ppm for **1** and **2** respectively.

The positive ion fast atom bombardment (FAB) mass spectra of **1** and **2** show peaks with $m/z = 1084$ and 1099 that correspond to molecular cations, as well as peaks that correspond to products of a successive fragmentation of these compounds.

A specific feature of the mass spectrum of complex **1** is the occurrence of a high-intensity peak with $m/z = 1543.9$ for the adduct $[C_6H_4CH_2C_6H_4(AuPPh_3)_3]^+$. This is a rather standard result of the ion–molecular reaction in the gaseous phase; however, in our case it has an important parallel with solution chemistry of gold–cationic complexes, where the clusterization resulting in digold complexes with the structural fragment **A** is a well-established process [23].

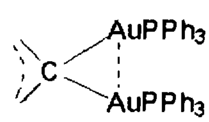

A

2.4. *Reactivity of complexes 1 and 2*

2.4.1. *Interaction of complex 1 with dppe*

In **1**, both PPh_3 ligands are readily replaced by the bidentate phosphine donor ligand dppe. At room temperature, the reaction of **1** with dppe in benzene is very quick and results in the precipitation of complex $\overline{Au(o\text{-}C_6H_4)CH_2(C_6H_4\text{-}o)Au(\mu\text{-}PPh_2CH_2CH_2PPh_2)}$ (**3**). This complex contains a macrocycle, in which two gold atoms interact with one another.

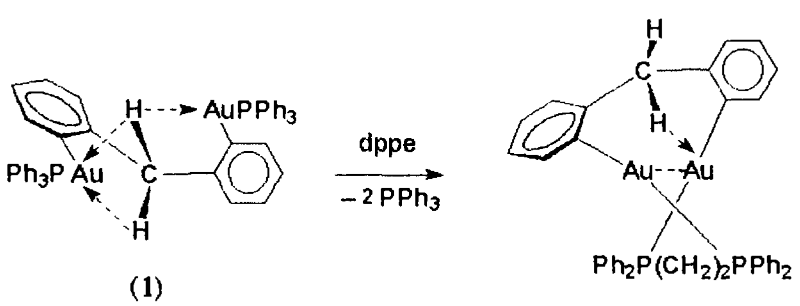

(**1**) (**3**), 95% (3)

The appropriate size for the bidentate diphosphine ligand was predicted by molecular mechanic calculation on a model molecule. The calculation demonstrates the complementary nature of the Au(o-C_6H_4)–CH_2–(o-C_6H_4)Au fragment of molecule **1** and the dppe molecule. The conformational flexibility of dppe is sufficient to form a macrocycle with the diaurated diphenylmethane fragment of **1** upon replacement of the two PPh_3 ligands. In the resultant macrocyclic molecule, a close arrangement of the two gold atoms is easily achieved.

An X-ray diffraction study of complex **3** (Fig. 3 and Table 2) reveals that the Au ··· Au distance (3.012 Å) is consistent with direct aurophilic interaction. The linear C–Au–P fragments are mutually rotated around the Au ··· Au vector. The C(1)Au(2) ··· Au(1)C(13) pseudo-torsion angle equals 55.6° (C_2 symmetry). Such an arrangement of two linear C–Au–P fragments was theoretically predicted to be necessary to achieve an Au ··· Au interaction [16].

The conformation of the 11-membered macrocycle is non-symmetric. The two structurally equivalent moieties of the macrocyclic molecule are geometrically different. The methylene hydrogen atoms of the organic ligand also occupy quite different positions with respect to the macrocycle: one of them, H(7A), is oriented towards the macrocycle and another, H(7B), on the opposite side. Only one gold atom, Au(1), approaches the H(7A) atom at the distance of 2.62 Å corresponding to an Au ··· H–C agostic bond. The distance to the second gold atom, Au(2), is too long (3.2 Å).

The macrocycle in **3** is somewhat strained as indicated by the following geometrical distortions.

(1) A significant deviation of the Au(1) atom (by 0.173 Å) from the plane of the C(1) ··· C(6) aryl ring towards the Au(2) atom is observed, whereas the second gold atom, Au(2), deviates from the plane of the second aryl ring only by 0.037 Å.

(2) The C–Au–P bond angle at the Au(2) atom is reduced and equals 168.6(4)° (instead of the ideal 180°); the angle opposite the Au(1) atom is reduced. The corresponding bond angle at the Au(1) atom (179.0(5)°) approximates to the ideal value.

We were interested in the nature of the geometrical distortions of the macrocyclic molecule **3**. Computer simulations based on the molecular mechanics method have shown that locking of the macrocycle can easily be achieved without the aforementioned distortions. Therefore, we suggest that these distortions result from a tendency to form a maximum number of secondary bonds with an optimally favorable geometry in this molecular system.

2.4.2. *Interaction of complexes 1 and 2 with [$AuPPh_3$]BF_4*

Digold-containing derivatives of diphenylmethane **1** and diphenylethane **2** readily react with the coordinationally unsaturated complex [$AuPPh_3$]BF_4 (prepared in situ from $ClAuPPh_3$ and $AgBF_4$) in THF to give cationic organogold complexes (**4–6**) of a new type, containing three and four gold atoms in the molecule, in high

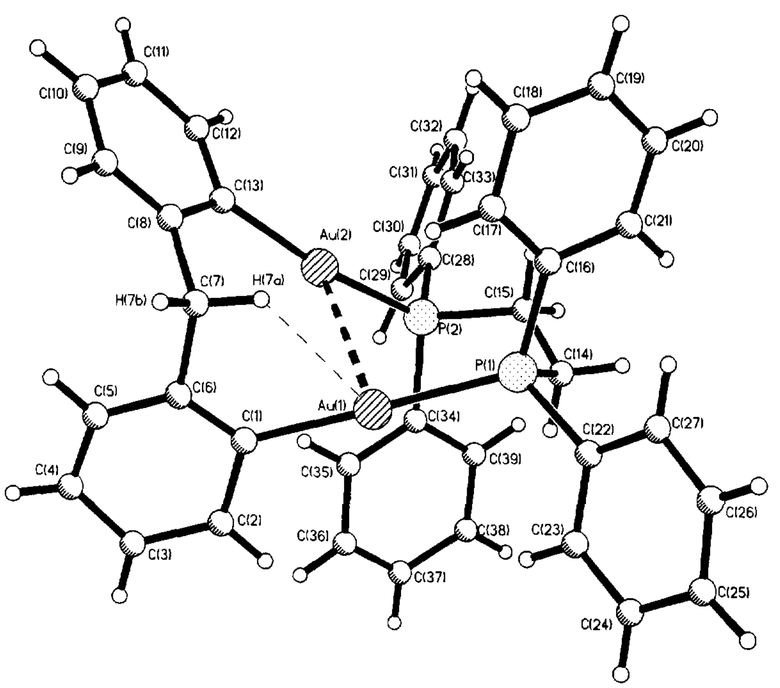

Fig. 3. The molecular structure of Au(o-C_6H_4)CH_2(C_6H_4-o)Au(μ-$PPh_2CH_2CH_2PPh_2$) (**3**).

yields. Depending on the ratio of the reagents, the reaction of the 2,2′-diphenylmethane derivative of gold **1** with $[AuPPh_3]BF_4$ leads to a mono- (**4**) or dicationic (**5**) organogold *ortho* derivative of diphenylmethane. Upon reaction of the 2,2′-diphenylethane complex **2** with two equivalents of $[AuPPh_3]BF_4$, a new dicationic tetranuclear organogold derivative of diphenylmethane **6** was synthesized.

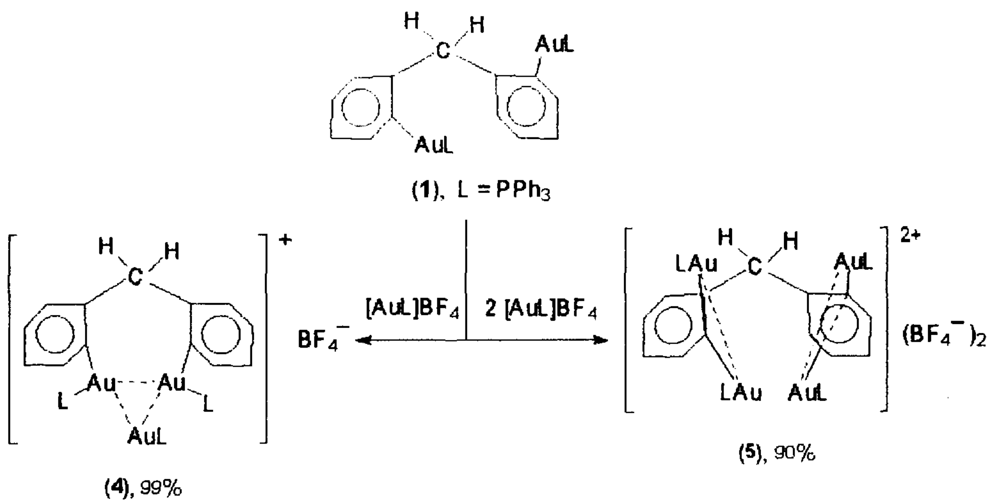

(4)

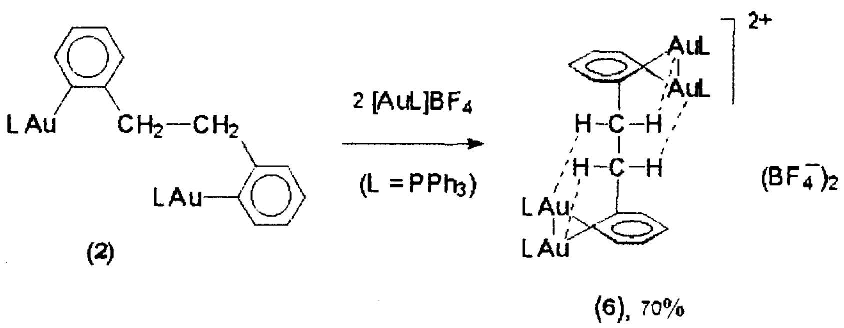

(5)

Complexes **4**–**6** are white, crystalline compounds, soluble in polar solvents, insoluble in water, and air-stable in the solid state.

The structure of the cationic complex **6** was determined using X-ray diffraction analysis, and for **4**–**6** by IR, ^1H and ^{31}P NMR spectroscopy and FAB MS, the formulations were also supported by elemental analyses.

Unfortunately, the rather low stability of **4** and **5** in solutions prevented the growth of single crystals suitable for X-ray diffraction study. The X-ray molecular structure of the cation of complex **6** is shown in Fig. 4; selected bond lengths and bond angles are listed in Table 3.

The *anti* conformation of the central ethylene fragment is dictated by the crystallographically found centrosymmetric nature of **6**. One *ortho* position of every aryl ring of the organic ligand turns out to be doubly aurated; that is, molecule **6** represents a dication. The BF_4^- anions act as counterions. The electron deficient triangles Au_2C are arranged in a perpendicular fashion to the plane of the corresponding aryl rings. The Au ··· Au distance in the triangle is 2.727(3) Å (the Au ··· Au distance in gold metal equals 2.88 Å). The AuCAu angle is 79.3(5)°. The Au(1) and Au(2) atoms are differently displaced from the plane of the aryl ring: by 1.503 and 1.208 Å respectively.

The aryl rings of the diphenylethane fragment are essentially planar. The conformation of the ligand in **6** resembles that in **2**. However, the occurrence of two rather than one gold atoms at each of the atoms C(1) and C(1a) of aryl rings, and the specific geometry of the Au_2C fragments, significantly changes the pattern of the weak agostic bonds. The system of such interactions is also shown in Fig. 4.

In the crystal structure of **6**, each of the four gold atoms is involved in its own Au ··· H–C agostic interaction, each of four hydrogen atoms of the $-CH_2-CH_2-$ bridge participating in these interactions. The Au ··· H distances are 2.6 and 3.0 Å.

The IR spectrum of the tetranuclear complex **6** in the solid state exhibits absorption bands for stretching vibrations of the CH bonds significantly shifted to a low frequency region (2690 cm^{-1}) compared with those in diphenylethane, a fact which provides support for the occurrence of the agostic bonds in **6**.

The ^1H NMR spectrum of **6** in CD_2Cl_2 contains complex multiplets from the aromatic protons and sharp singlets (at room temperature) from the protons of the

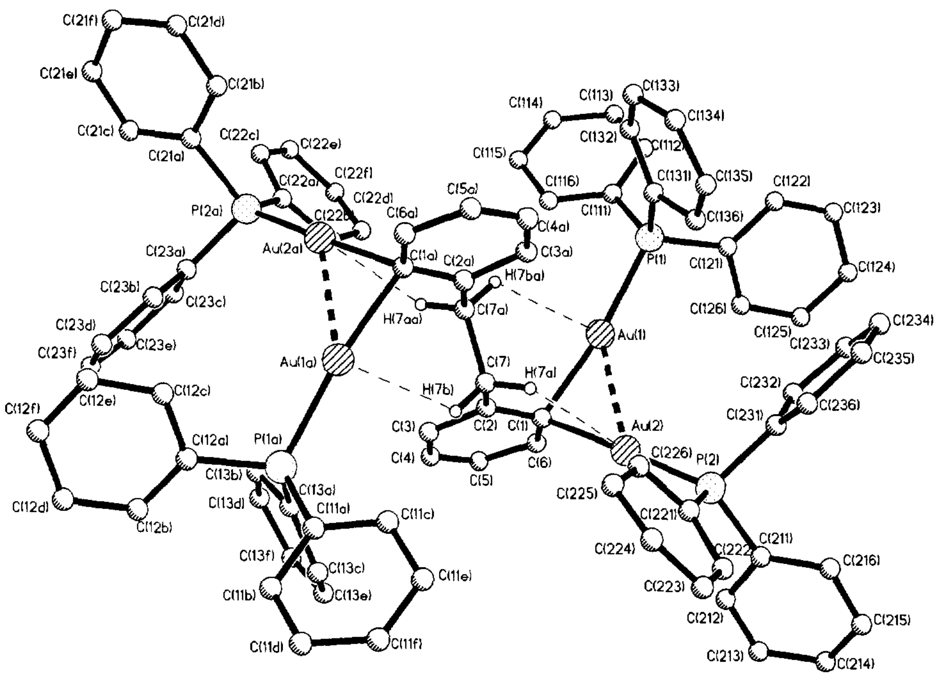

Fig. 4. The molecular structure of the cation $[(CH_2)_2(C_6H_4\text{-}o)_2[AuPPh_3)_4]$ (**6**). All hydrogen atoms except those at the C(7) and C(7a) atoms are omitted.

bridging $(CH_2)_2$ groups (3.52 ppm). A cooling of the sample of complex **6** to −95 °C is accompanied by a significant broadening of the signal from protons of the ethylene group and its low field shift (3.57 ppm), a fact which shows the dynamic behavior of **6**, the nature of which is not yet clearly understood.

The ^{31}P NMR spectrum of complex **6** in CD_2Cl_2 solution at +25 to −95 °C displays a sharp signal from the four equivalent phosphorus atoms (32.82 ppm).

The ^{1}H NMR spectra of **4** and **5** in CD_2Cl_2 contain complex multiplets from the aromatic protons and sharp singlets (at room temperature) from the protons of the CH_2 bridge (4.37 ppm for **4** and 3.97 ppm for **5**).

The temperature dependence of the ^{31}P NMR spectra of the tri- and tetragold-containing derivatives of diphenylmethane **4** and **5** within the range +25 to −95 °C allowed us to observe their conformational non-rigidity in solution (CD_2Cl_2). The spectrum of complex **4** at +25 °C exhibits a sharp singlet from the three equivalent phosphorus nuclei (37.80 ppm). On cooling the solution to −95 °C, a significant broadening of this signal occurs. This indicates that in solution a rotation around the single C–C bonds occurs simultaneously with rapid intramolecular exchanges due to transfer between the gold-containing groups of cation **4** (Eq. (6)).

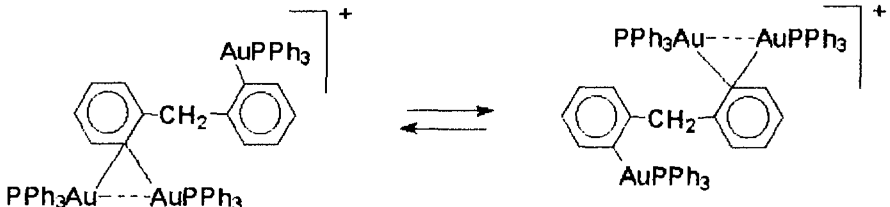

4 **4** (6)

The ^{31}P NMR spectrum of the tetranuclear complex **5** in CD_2Cl_2 at +25 °C exhibits a sharp signal (36.31 ppm). However, starting from −45 °C and down to −95 °C this signal resolves into two sharp signals. The decrease in temperature results in a slowing down of the hindered rotation of the bulky digold-containing phenyl rings around the exocyclic C–C single bonds, and affords the most preferable conformation of complex **5** (Fig. 5). In this conformation, the two $AuPPh_3$ groups of a common $[C(AuPPh_3)_2]^+$ fragment appear to be non-equivalent.

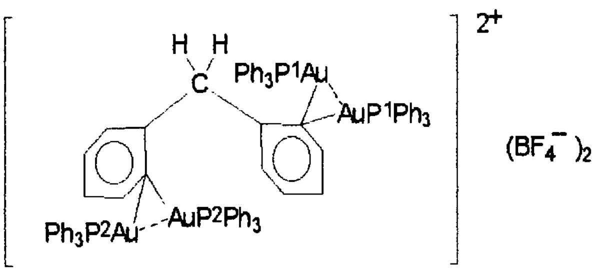

5

One of them is directed towards the bridging CH_2 group, whereas the other is directed away from it. At low temperatures, the conformation of **5** with two pairs of equivalent phosphorus atoms of the PPh_3 ligand is frozen out. The energy barrier of the rotation around the exocyclic C–C bond (calculated on the basis of parameters of the ^{31}P NMR spectra of **5** recorded at 5° intervals), $\Delta G^{\#}_{235\,K}$, is $10.8 \pm 0.4\,kcal\,mol^{-1}$ ($\Delta H^{\#} = 9.4 \pm 0.4\,kcal\,mol^{-1}$ and $\Delta S^{\#} = -5.8 \pm 0.9\,cal\,mol^{-1}\,K$). A low entropy of the process is indicative of a high

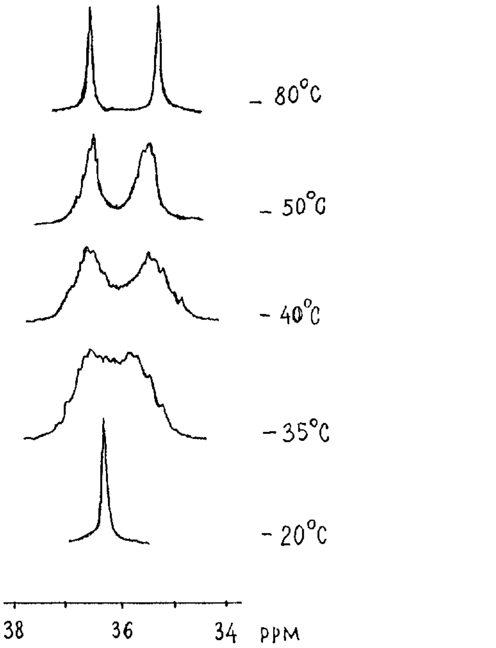

Fig. 5. Variable temperature ^{31}P NMR spectra of complex **5** in the range +25 to −95°C (in CD_2Cl_2).

ordering in the molecule and predominance of a single conformation for complex **5**.

The interaction of tetranuclear gold complex **5** with PPh_3 brings about easy generation of the dinuclear gold derivative **1** and formation of $[(Ph_3P)_2Au]BF_4$.

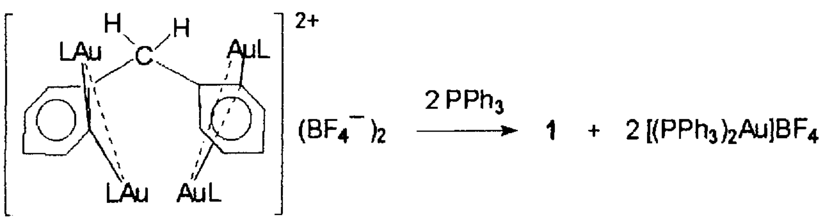

5 (L = PPh_3)

(7)

3. Experimental

3.1. Instrumentation

The IR spectra were recorded on a UR-20 instrument (KBr), ^1H NMR spectra on a Bruker WP-200SY (200 MHz), and ^{31}P spectra on a Bruker CXP_6 200 (81 MHz) using 85% H_3PO_4 as external standard. The FAB mass spectra were recorded on a Kratos concept instrument using a fast atom (Cs) bombardment energy of 8 keV and 3-nitrobenzyl alcohol as matrix.

3.2. X-ray diffraction analysis of 2, 3 and 6

Crystals of **2**, **3** and **6** suitable for X-ray diffraction study were grown from CH_2Cl_2, C_6H_6 and $CHCl_3$ respectively. The main crystallographic and data collection parameters as well as structure refinement conditions are summarized in Table 4. The unit cell parameters and experimental reflections were measured on an Enraf–Nonius CAD-4 diffractometer (Mo Kα radiation, graphite monochromator) at room temperature for **3** and at −100 °C for **2** and **6**. The $\omega/2\theta$ (for **3**) and ω (for **2** and **6**) scan techniques were used.

All the structures were solved by the heavy-atom method and refined by full-matrix least-squares in the isotropic approximation. At this stage of the refinement, the absorption correction was taken into account by applying the DIFABS method [24].

Final structure refinement of **3** was carried out in the anisotropic approximation for non-hydrogen atoms ex-

Table 2
Selected bond lengths (*d*, Å) and angles (*ω*, deg) for **3**

Bond	*d*
Au(1)–C(1)	2.04(2)
Au(1)–P(1)	2.296(5)
Au(1)–Au(2)	3.012(2)
Au(2)–C(13)	2.05(2)
Au(2)–P(2)	2.296(4)
Au(1) · · · H(7a)	2.62
C(1)–C(6)	1.26(3)
C(1)–C(2)	1.47(2)
C(2)–C(3)	1.45(4)
C(3)–C(4)	1.37(3)
C(4)–C(5)	1.36(3)
C(5)–C(6)	1.33(3)
C(6)–C(7)	1.57(2)
C(7)–C(8)	1.57(2)
C(8)–C(9)	1.34(2)
C(8)–C(13)	1.43(2)
C(9)–C(10)	1.37(3)
C(10)–C(11)	1.37(2)
C(11)–C(12)	1.35(3)
C(12)–C(13)	1.38(2)
Angle	***ω***
C(1)–Au(1)–P(1)	179.0(5)
C(1)–Au(1)–Au(2)	82.2(5)
P(1)–Au(1)–Au(2)	96.8(1)
C(13)–Au(2)–P(2)	168.6(4)
C(13)–Au(2)–Au(1)	106.7(4)
P(2)–Au(2)–Au(1)	84.47(11)
C(6)–C(1)–C(2)	114(2)
C(6)–C(1)–Au(1)	127(1)
C(2)–C(1)–Au(1)	119(2)
C(3)–C(2)–C(1)	121(2)
C(4)–C(3)–C(2)	119(2)
C(5)–C(4)–C(3)	115(2)
C(6)–C(5)–C(4)	126(2)
C(1)–C(6)–C(5)	125(2)
C(1)–C(6)–C(7)	118(2)
C(5)–C(6)–C(7)	117(2)
C(6)–C(7)–C(8)	115(1)
C(9)–C(8)–C(13)	122(2)
C(9)–C(8)–C(7)	120(1)
C(13)–C(8)–C(7)	118(1)
C(8)–C(9)–C(10)	122(2)
C(11)–C(9)–C(10)	118(2)
C(12)–C(11)–C(10)	120(2)
C(11)–C12)–C(13)	124(1)
C(12)–C(13)–C(8)	114(1)
C(12)–C(13)–Au(2)	117(1)
C(8)–C(12)–Au(2)	129(1)

cept carbon atoms of the solvent benzene molecules. In structures **2** and **6**, only heavy atoms (Au, P and Cl of the CH_2Cl_2 solvent molecule in **2** and Au and P in **6**) were refined anisotropically. In these structures, because of a poor data/parameter ratio, all Ph rings were refined using geometrical restraints to make chemically equivalent distances equal. The 1,2, 1,3 and 1,4 distances in the rings were assumed to be equal to 1.39, 2.42 and 2.80 Å respectively, with an estimated standard deviation of 0.03 Å. Hydrogen atom positions were calculated based on standard values of the C–H bond lengths and CCH (as well as HCH) bond angles and included in the refinement using the 'riding' scheme.

In all structures, the peaks of residual electron density are located in the vicinity of the gold atoms or (in **6**) the disordered BF_4 anion. The high values of these peaks are due to the rather small number of experimental reflections obtained.

All of the calculations were performed using the SHELX-76 and SHELX-93 software in the laboratory of Professor J.A.K. Howard (Chemistry Department, Durham University, Durham, UK).

Detailed crystallographic data can be obtained from the authors.

3.3. Synthesis of complexes

Complexes **1–3** were synthesized under dry argon using solvents pre-distilled over benzophenonesodium ketyl in argon atmosphere.

Table 3
Selected bond lengths (*d*, Å) and angles (*ω*, deg) for **6**

Bond	*d*
Au(1)–C(1)	2.13(4)
Au(1)–P(1)	2.27(1)
Au(1)–Au(2)	2.727(3)
Au(2)–C(1)	2.12(4)
Au(2)–P(2)	2.26(1)
Au(1) · · · H(7ba)	3.0
Au(2) · · · H(7a)	2.6
C(1)–C(2)	1.33(5)
C(1)–C(6)	1.45(5)
C(2)–C(3)	1.44(6)
C(2)–C(7)	1.42(6)
C(3)–C(4)	1.42(6)
C(4)–C(5)	1.27(5)
C(5)–C(6)	1.45(5)
C(7)–C(7A)	1.51(9)
Angle	***ω***
C(1)–Au(1)–P(1)	172(1)
C(1)–Au(1)–Au(2)	50(1)
P(1)–Au(1)–Au(2)	137.1(3)
C(1)–Au(2)–P(2)	172(1)
C(1)–Au(2)–Au(1)	50(1)
P(2)–Au(2)–Au(1)	132.6(3)
C(2)–C(1)–C(6)	116(4)
C(2)–C(1)–Au(1)	113(3)
C(6)–C(1)–Au(1)	106(3)
C(2)–C(1)–Au(2)	120(3)
C(6)–C(1)–Au(2)	116(3)
Au(1)–C(1)–Au(2)	80(1)
C(1)–C(2)–C(3)	119(4)
C(1)–C(2)–C(3)	120(4)
C(1)–C(2)–C(7)	120(4)
C(3)–C(2)–C(7)	120(4)
C(4)–C(3)–C(2)	120(4)
C(5)–C(4)–C(3)	124(4)
C(4)–C(5)–C(6)	116(4)
C(1)–C(6)–C(5)	125(3)
C(7A)–C(7)–C(2)	115(7)

The formations of **1** and **2** were monitored by TLC on Silufol (in benzene).

3.3.1. Preparation of $Ph_3PAu(o\text{-}C_6H_4)CH_2(C_6H_4\text{-}o)AuPPh_3$ (1)

2.85 M hexane solution of ^nBuLi in 15 ml ether was added dropwise to a solution of 2,2′-diiododiphenylmethane (3.30 g, 7.86 mmol) in 60 ml of ether at 0 °C under vigorous stirring. The reaction mixture was stirred for 4 h at room temperature. Then, 2.63 g (5.31 mmol) of $ClAuPPh_3$ in 60 ml of THF was poured into the agitated suspension in small portions. After the disappearance of a mixture of the gold halide complexes ($ClAuPPh_3$ and $IAuPPh_3$ – the latter forming from $ClAuPPh_3$ in the course of the reaction) from the reaction mixture, the reaction solution was decomposed in water. The organic layer was dried with K_2CO_3 and evaporated to a volume of around 5 ml. Compound **1** (1.84 g, 64%) was precipitated from the solution after addition of ether, m.p. 186–187 °C (decomp.) after reprecipitation with ether–hexane mixture (1:1) from the benzene solution. Anal. Found: C, 54.26; H, 3.73; P, 5.81. $C_{49}H_{40}Au_2P_2$ Calc.: C, 54.25; H, 3.71; P, 5.71%. IR (ν, cm^{-1}): 3155 m, 2995 w, 2910 w, 2882 w, 2800 w, 2740 w, 2685 w, 1587 w, 1310 w, 1183 w, 1111 m, 1042 w, 1010 w, 755 s, 742 m, 730 m, 708 m, 535 m, 522 m.

3.3.2. Preparation of $Ph_3PAu(o\text{-}C_6H_4)(CH_2)_2(C_6H_4\text{-}o)AuPPh_3$ (2)

A suspension of 2,2′-dilithiodiphenylethane (prepared according to the procedure described in Ref. [25] from

Table 4
Crystal data and structure refinement details for **2**, **3** and **6**

	2	3	6
Crystal parameters			
Formula	$(C_{50}H_{42}Au_2P_2)\cdot CH_2Cl_2$	$(C_{39}H_{34}Au_2P_2)\cdot 2C_6H_6$	$(C_{86}H_{72}Au_4P_4)2BF_4\cdot CHCl_3$
Formula weight	1183.7	1114.8	1579.9
Crystal system	monoclinic	monoclinic	triclinic
Crystal color; habit	colorless; plate	colorless; block	colorless; block
Crystal size (mm^3)	0.06 × 0.09 × 0.12	0.9 × 0.8 × 0.7	0.12 × 0.08 × 0.10
Space group	$P2_1/c$	$P2_1$	$P1$
a (Å)	11.155(9)	9.484(10)	10.555(2)
b (Å)	7.568(10)	18.047(8)	13.125(3)
c (Å)	27.056(7)	12.745(9)	17.210(3)
α (deg)	90	90	71.10(3)
β (deg)	96.22(5)	99.47(5)	82.07(3)
γ (deg)	90	90	73.77(3)
V (Å^3)	2270(1)	2152(3)	2162.8(7)
Z	2	2	1
D_c ($g\,cm^{-3}$)	1.731	1.721	1.774
$F(000)$	1144	1080	1104
μ(Mo Kα) (mm^{-1})	6.66	6.90	6.98
T (K)	173	293	293
Data collection and refinement (Mo Kα, λ = 0.71073 Å)			
Scan mode	ω	$\omega/2\theta$	ω
Scan speed (deg min^{-1})	16.0 (in ω)	16.0 (in ω)	16.0 (in ω)
Scan range ω	1.0 + 0.35 tan q	1.2 + 0.35 tan q	1.2 + 0.35 tan q
θ range (deg)	2.80 to 25.43	2.18 to 27.94	2.01 to 22.95
Index ranges	$-13 < h < 13$	$-12 < h < 12$	$-11 < h < 11$
	$0 < k < 9$	$0 < k < 13$	$-13 < k < 12$
	$0 < l < 32$	$0 < l < 16$	$0 < l < 17$
Reflections collected	1609	3176	1574
Independent reflections	1609 [$R(f)$ = 0.000]	3176 [$R(f)$ = 0.000]	1574 [$R(f)$ = 0.000]
Absorption correction	DIFABS	DIFABS	DIFABS
Max. and min. transmission	0.987/0.760	0.946/0.683	0.867/0.523
Refinement method (on F^2)	full-matrix least-squares	full-matrix least-squares	full-matrix-block least-squares
Data/restraints/parameters	1606/62/133	3161/1/438	1572/90/254
Goodness-of-fit	1.165	1.045	1.018
Final R indices [$I > 2\sigma(I)$]	R_1 = 0.0796	R_1 = 0.0577	R_1 = 0.0725
	wR_2 = 0.2072	wR_2 = 0.1542	wR_2 = 0.1877
Extinction coefficient	0.0062(11)	0.0000(2)	0.0008(3)
Largest difference peak and hole (e Å^{-3})	3.775 and −3.281	3.314 and −3.715	1.746 and −2.014
Flack x parameter		0.00(3)	

2.04 g (6 mmol) of 2,2′-dibromodiphenylethane in 12 ml of ether and 5.90 ml (12.80 mmol) of 2.17 M hexane solution of ^{n}BuLi in 12 ml of ether) was added dropwise to a suspension of 2.00 g (4.00 mmol) of $ClAuPPh_3$ in 45 ml of THF upon stirring for 2 h. The reaction mixture was decomposed with water. The organic layer was dried with K_2CO_3 and boiled down to a volume of around 5 ml. The precipitate was separated, treated with ether (2 × 10 ml) and dried. After reprecipitation from the THF solution with ether–petroleum ether (1:1) mixture, the yield of **2** was 1.03 g (47%), m.p. 206–208 °C (decomp.). Anal. Found: C, 54.16; H, 3.97; P, 5.82. $C_{50}H_{42}Au_2P_2$ Calc.: C, 54.65; H, 3.85; P, 5.64%. IR (ν, cm^{-1}): 3060 m, 2932 m, 2842 w, 2740 w, 2590 w, 1590 w, 1333 w, 1312 w, 1274 w, 1189 w, 1170 w, 1103 m, 1032 m, 1002 w, 941 w, 849 w, 755 m, 732 m, 715 m, 700 m, 540 m, 508 m.

From the mother liquor, 0.08 g of **2** was additionally isolated. The total yield of **2** was 1.11 g (51%).

*3.3.3. Interaction of $Ph_3PAu(o\text{-}C_6H_4)CH_2(C_6H_4\text{-}o)AuPPh_3$ (**1**) with dppe*

A solution of dppe (0.17 g, 0.43 mmol) in 10 ml of benzene was added to a solution of **1** (0.48 g, 0.43 mmol) in 20 ml of benzene. A crystalline precipitate was separated, washed with pentane (4 × 5 ml), and dried. The yield of μ-diphenylphosphinoethane-bis-aurio(2,2′-diphenylmethane) (**3**) was 0.39 g (95%), m.p. 260–262 °C. Anal. Found: C, 48.75; H, 3.30. $C_{39}H_{34}Au_2P_2$ Calc.: C, 48.86; H, 3.37%. ^{1}H NMR spectrum (CD_2Cl_2, δ, ppm): 2.80 (d, ^2J(P–H) 12 Hz, 4H, dppe), 4.45 (s, 2H), 7.05–7.08 (m, 28H). ^{31}P NMR spectrum (CD_2Cl_2, δ, ppm): 35.34 (s). FAB MS, m/z: 959 $[M]^+$.

*3.3.4. Preparation of $[CH_2(C_6H_4\text{-}o)_2(AuPPh_3)_3]BF_4$ (**4**)*

A solution of $[AuPPh_3]BF_4$ (prepared from 0.11 g (0.22 mmol) of $ClAuPPh_3$ and 0.105 g (0.23 mmol) of $AgBF_4 \cdot 3$dioxane in 10 ml of THF at −60 °C) was added to a solution of **1** (0.20 g, 0.185 mmol) in 15 ml of THF. Within 5 min, the reaction solution was diluted with cooled ether to turbidity. Within 15 min, the precipitate was filtered off, washed with cold ether, and dried. The yield was 0.30 g (a quantitative yield), m.p. 185 °C (decomp.). Anal. Found: C, 49.31; H, 3.29; P, 5.87. $C_{67}H_{55}Au_3BF_4P_3$ Calc.: C, 49.34; H, 3.40; P, 5.70%. IR (ν, cm^{-1}): 3048 w, 2990 m, 2780 w, 2690 w, 1606 w, 1102 m, 1060 s, 1028 m, 1000 m, 756 m, 746 m, 710 m, 697 m, 534 m, 512 m.

*3.3.5. Preparation of $[CH_2(C_6H_4\text{-}o)_2(AuPPh_3)_4](BF_4)_2$ (**5**)*

A solution of $[AuPPh_3]BF_4$ (prepared from $ClAuPPh_3$ (0.22 g, 0.44 mmol) and $AgBF_4 \cdot 3$ dioxane (0.21 g, 0.46 mmol) in 20 ml of THF) was added to a solution of **1** (0.20 g, 0.185 mmol) in 15 ml of THF at −60 °C. The reaction solution was stirred for 30 min at −60 °C and allowed to remain for 15 min at −10 °C. The precipitate was separated, washed with THF (2 × 3 ml), and dried. The yield of **5** was 0.36 g (90%), m.p. 185 °C (decomp.). Anal. Found: C, 46.64; H, 2.98; P, 6.05. $C_{85}H_{70}Au_4B_2F_8P_4$ Calc.: C, 46.89; H, 3.24; P, 5.69%. IR (ν, cm^{-1}): 3060 w, 2985 m, 2922 m, 2890 m, 2690 w, 1146 w, 1103 m, 1064 s, 1035 m, 1002 w, 870 w, 755 m, 732 m, 700 m, 542 m, 515 m, 502 m.

*3.3.6. Preparation of $[(CH_2)_2(C_6H_4\text{-}o)_2(AuPPh_3)_4](BF_4)_2$ (**6**)*

A solution of $[AuPPh_3]BF_4$ (prepared from $ClAuPPh_3$ (0.19 g, 0.37 mmol) and $AgBF_4$ (0.08 g, 0.41 mmol) in 10 ml of THF) was added to a suspension of **2** (0.20 g, 0.186 mmol) in 30 ml of THF upon vigorous agitation at −15 °C. Complete dissolution of **6** was first observed, followed by precipitation of a white compound. Within 1 h, 400 ml of ether at −15 °C was added to the suspension formed. The precipitate was separated and dried. The yield of **6** was 0.25 g (62%), m.p. 174–175 °C (after reprecipitation from THF with ether). Anal. Found: C, 46.58; H, 3.29; P, 6.00. $C_{86}H_{72}Au_4B_2F_8P_4$. Calc.: C, 47.14; H, 3.31; P, 5.65%.

From the mother liquor, 0.03 g of **6** was additionally isolated. The total yield of **6** was 0.28 g (70%).

*3.3.7. Interaction of complex **5** with PPh_3*

A solution of PPh_3 (0.08 g, 0.30 mmol) in 1.5 ml of acetone was added to a suspension of **5** (0.10 g, 0.046 mmol) in 3 ml of acetone at −20 °C. After 20 min reduction at −20 °C, the reaction mixture was evaporated in vacuo to dryness. The residue was washed with pentane (4 × 4 ml) and treated with benzene (4 × 3 ml). The benzene extracts were diluted with excess petroleum ether. The precipitate was separated out and washed with pentane. The yield of **1** was 0.05 g (99%), m.p. 186 °C (decomp.) (after reprecipitation from benzene with excess petroleum ether).

After the extraction with benzene, the solid residue was reprecipitated from the acetone solution with ether–pentane (1:1) mixture. The yield of $[(Ph_3P)_2Au]BF_4$ was 0.05 g (71%), m.p. 234–236 °C (from the CH_3OH–hexane mixture). Literature data 234–235 °C [26].

Acknowledgements

We are indebted to Drs. P.V. Petrovskii and M.V. Galakhov for recording the NMR spectra, and D.V. Zagorevskii and K.V. Kazakov for recording the mass spectra. This work was supported by Grant No. MDV300 from the International Science Foundation and the Russian Government, as well as by the Russian Foundation for Fundamental Research, Project No. 95-03-08616a.

References

[1] L.G. Kuz'mina, N.V. Dvortsova, M.A. Porai-Koshits, E.I. Smyslova, K.I. Grandberg and E.G. Perevalova, *Metalloorg. Khim., 2* (1989) 1344.
[2] L.G. Kuz'mina, N.V. Dvortsova, O.Yu. Burtseva, M.A. Porai-Koshits, E.I. Smyslova and K.I. Grandberg, *Metallorg. Khim., 3* (1990) 364.
[3] L.G. Kuz'mina, *Neorg. Khim., 37* (1992) 1773.
[4] L.G. Kuz'mina, N.V. Dvortsova, O.Yu. Burtseva and M.A. Porai-Koshits, *Metalloorg. Khim., 2* (1989) 1242.
[5] M.K. Cooper, K. Henrick, M. McPartlinand and L. Latten, *Inorg. Chim. Acta, 65*(5) (1982) L185.
[6] T.V. Baukova, Yu.L. Slovokhotov and Yu.T. Struchkov, *J. Organomet. Chem., 220* (1981) 125.
[7] M.I. Bruce, J.K. Walton, B.W. Skelton and A.H. White, *J. Chem. Soc., Dalton Trans.*, (1983) 809.
[8] H. Werner, H. Otto, T. Ngo-Khaa and C. Burschka, *J. Organomet. Chem., 262* (1984) 123.
[9] T.V. Baukova, Yu.L. Slovokhotov and Yu.T. Struchkov, *J. Organomet. Chem., 221* (1981) 375.
[10] S. Gambarotta, B. Floriani, A. Chiesi-Villa and C. Guastini, *J. Chem. Soc., Chem. Commun.*, (1983) 1305.
[11] V.G. Andrianov, Yu.T. Struchkov and E.R. Rosinskaya, *J. Chem. Soc., Chem. Commun.*, (1973) 339.
[12] L.G. Kuz'mina, *Neorg. Khim., 38* (1993) 994.
[13] H. Schmidbaur, W. Graf and G. Muller, *Angew. Chem., Int. Ed. Engl., 27* (1988) 417.
[14] Md Zi Khan, J.P. Fackler, Jr., Ch. King, J.C. Wang and S. Wang, *Inorg. Chem., 27* (1988) 1672.
[15] K.M. Merz, Jr. and R. Hoffmann, *Inorg. Chem., 27* (1988) 2120.
[16] P. Pyykko and Y. Zhao, *Angew. Chem., Int. Ed. Engl., 30* (1991) 604.
[17] J. Li and P. Pyykko, *Inorg. Chem., 32* (1993) 2630.
[18] V.P. Dyadchenko, P.E. Krasik, K.I. Grandberg, L.G. Kuz'mina, N.V. Dvortsova, M.A. Porai-Koshits and E.G. Perevalova, *Metalloorg. Khim., 3* (1990) 654.
[19] T.V. Baukova, H.N. Oleinikova, D.A. Lemenovskii and L.G. Kuz'mina, *Izv. Akad. Nauk, Ser. Khim.*, (1994) 729 [*Russ. Chem. Bull., 43*(4) (1994) 1 (Engl. transl.)].
[20] T.V. Baukova, V.P. Dyadchenko, N.A. Oleinikova, D.A. Lemenovskii and L.K. Kuz'mina, *Izv. Akad. Nauk, Ser. Khim.*, (1994) 1125 [*Russ. Chem. Bull., 43*(6) (1994) 1063].
[21] A.A. Bagatur'yants, *Itogi Nauki I Tekhniki; Kinetika I Kataliz*, Vol. 14, VINITI, Moscow, 1985.
[22] M. Brukhart and M.L.H. Green, *J. Organomet. Chem., 250* (1983) 395.
[23] A.N. Nesmeyanov, E.G. Perevalova, K.I. Grandberg, D.A. Lemenovskii, T.V. Baukova and O.B. Afanasova, *J. Organomet. Chem., 65* (1974) 131.
[24] N. Walker and D. Stuart, *Acta Crystallogr., 39A* (1983) 158.
[25] R.L. Letsinger, J.H. Skoog and N. Rences, *J. Am. Chem. Soc., 77* (1955) 5176.
[26] K.I. Grandberg, T.V. Baukova, E.G. Perevalova and A.N. Nesmeyanov, *Dokl. AN SSSR, 206* (1972) 1355.